EBioMedicine 5 (2016) 82–92

Contents lists available at ScienceDirect

EBioMedicine

journal homepage: www.ebiomedicine.com

Research Paper

# The Ablation of Mitochondrial Protein Phosphatase Pgam5 Confers Resistance Against Metabolic Stress

Shiori Sekine [a,1], Akari Yao [a,1], Kazuki Hattori [a], Sho Sugawara [a], Isao Naguro [a], Masato Koike [b], Yasuo Uchiyama [c], Kohsuke Takeda [d], Hidenori Ichijo [a,*]

[a] Laboratory of Cell Signaling, Graduate School of Pharmaceutical Sciences, The University of Tokyo, Tokyo, Japan
[b] Department of Cell Biology and Neuroscience, Juntendo University Graduate School of Medicine, Tokyo, Japan
[c] Departments of Cellular and Molecular Neuropathology, Juntendo University Graduate School of Medicine, Tokyo, Japan
[d] Division of Cell Regulation, Graduate School of Briomedical Sciences, Nagasaki University, Nagasaki, Japan

ARTICLE INFO

*Article history:*
Received 10 November 2015
Received in revised form 24 January 2016
Accepted 26 January 2016
Available online 29 January 2016

*Keywords:*
Mitochondria
Stress response
Metabolic stress
Obesity
FGF21

ABSTRACT

Phosphoglycerate mutase family member 5 (PGAM5) is a mitochondrial protein phosphatase that has been reported to be involved in various stress responses from mitochondrial quality control to cell death. However, its roles *in vivo* are largely unknown. Here, we show that Pgam5-deficient mice are resistant to several metabolic insults. Under cold stress combined with fasting, Pgam5-deficient mice better maintained body temperature than wild-type mice and showed an extended survival rate. Serum triglycerides and lipid content in brown adipose tissue (BAT), a center of adaptive thermogenesis, were severely reduced in Pgam5-deficient mice. Moreover, although Pgam5 deficiency failed to maintain proper mitochondrial integrity in BAT, it reciprocally resulted in the dramatic induction of fibroblast growth factor 21 (FGF21) that activates various functions of BAT including thermogenesis. Thus, the enhancement of lipid metabolism and FGF21 may contribute to the cold resistance of Pgam5-deficient mice under fasting condition. Finally, we also found that Pgam5-deficient mice are resistant to high-fat-diet-induced obesity. Our study uncovered that PGAM5 is involved in the whole-body metabolism in response to stresses that impose metabolic challenges on mitochondria.



## 1. Introduction

Phosphoglycerate mutase family member 5 (PGAM5) is a mitochondria-resident protein that belongs to the PGAM family, an evolutionarily conserved enzyme family. Prototypical PGAM family member proteins function in glycolysis as mutases (Jedrzejas, 2000). Although the amino acid sequence of the catalytic core of other PGAM family members is conserved in PGAM5, we previously reported that PGAM5 lacks mutase activity and instead acts as a Ser/Thr-specific protein phosphatase (Takeda et al., 2009). Although a previous report suggested that PGAM5 is targeted to the outer mitochondrial membrane (OMM) (Lo and Hannink, 2008), we found that PGAM5 is mainly localized to the inner mitochondrial membrane (IMM) through its N-terminal transmembrane domain and is cleaved by presenilins-associated rhomboid-like protein (PARL), an IMM-resident intramembrane protease, in response to the loss of mitochondrial membrane potential (Sekine et al., 2012). Recently, it has been suggested that PGAM5 is involved in several stress responses at both the cellular and organelle levels, including apoptosis (Zhuang et al., 2013), necroptosis (Wang et al., 2012), and autophagic mitochondrial degradation (Chen et al., 2014; Lu et al., 2014). However, the physiological roles of PGAM5 *in vivo* are largely unknown, except for one report suggesting that Pgam5-deficient mice show late-onset Parkinson's disease-like phenotypes (Lu et al., 2014).

Mitochondria, in which PGAM5 resides, are the largest cellular energy store, housing OXPHOS proteins for ATP generation and β-oxidation enzymes for fuel delivery. When bodies are exposed to stresses that disrupt energy homeostasis, it is expected that several metabolic challenges are imposed on mitochondria. Among such metabolic stresses, mitochondria play important roles in cold resistance. Cold stress sympathetically activates brown adipose tissue (BAT), a center of heat production (Morrison et al., 2014). Heat generation in BAT requires the IMM-resident uncoupler UCP1, which dissipates chemical energy to heat, and this process is termed nonshivering adaptive thermogenesis (Krauss et al., 2005). Activated BAT burns lipids through β-oxidation to sustain heat production, which results in an increase in energy expenditure (Townsend and Tseng, 2014). In addition to UCP1, the ablation of components that are required for β-oxidation, such as carnitine

* Corresponding author.
*E-mail address:* ichijo@mol.f.u-tokyo.ac.jp (H. Ichijo).
[1] These authors contributed equally to this work.

http://dx.doi.org/10.1016/j.ebiom.2016.01.031

palmitoyl-transferase 1β (CPT1β) and acyl-CoA synthetase long-chain family member 1 (ACSL1), all of which are vulnerable to cold stress (Ellis et al., 2010; Enerback et al., 1997; Ji et al., 2008), emphasizes the importance of mitochondria for cold resistance. Several humoral factors also participate in the activation of BAT (Villarroya and Vidal-Puig, 2013). Among these factors, FGF21, the 21st member of the fibroblast growth factor (FGF) family (Nishimura et al., 2000), is induced by cold stress (Chartoumpekis et al., 2011; Hondares et al., 2011) and ultimately protects mice from cold (Fisher et al., 2012). Interestingly, several recent reports have suggested that FGF21 is also induced in response to mitochondrial dysfunction (Dogan et al., 2014; Kim et al., 2013a,b), raising the possibility that FGF21 can regulate whole-body energy expenditure when enormous metabolic challenges are imposed on mitochondria.

Here, we revealed that Pgam5 knockout (KO) mice are resistant to cold stress combined with fasting. Consistent with the knowledge that cold sensitivity is correlated with obese phenotype (Lin and Li, 2004), Pgam5 KO mice also showed a resistance against high-fat-diet-induced obesity. Our study uncovered that mitochondria-resident stress responsive molecule PGAM5 may act as a metabolic regulator *in vivo*.

## 2. Materials and Methods

### 2.1. Mice

The mice were housed in a specific pathogen-free facility. For fasting and cold stress, 9–11-week-old male mice were fasted for 12 h and subsequently kept in a cold room (4 °C) for the indicated time periods. For the HFD-induced obesity model, 4–5-week-old male mice were fed a HFD (High Fat Diet 32, CLEA Japan, Inc.) for the indicated time periods. Body temperature was measured using a BAT-12 (MUROMACHI KIKA I). All of the mouse experiments were performed in accordance with protocols approved by the Animal Research Committee of the Graduate School of Pharmaceutical Sciences at the University of Tokyo (Tokyo, Japan).

### 2.2. Generation of Pgam5 KO Mice

A targeting vector was constructed in which a 4.9-kb fragment of the Pgam5 gene, containing exons 1–5, was replaced by a reversed-oriented neomycin phosphotransferase cassette. An upstream 6.3-kb fragment and a downstream 3.9-kb fragment of this cassette were used as homologous arms for recombination (Figure S1a). A Not I-linearized targeting vector was electroporated into RENKA embryonic stem cells (Transgenic Inc., Japan) derived from C57BL/6 mice and subjected to selection with G418. After the disruption of the Pgam5 gene was confirmed by Southern blotting, established ES cells were injected into 8-cell-stage embryos of ICR mice. The germline transmission of the mutated allele to F1 mice, as obtained by an intercross of resulting male chimeras and female C57BL/6 mice, was confirmed by Southern blotting (Figure S1b). Homozygous mutant mice were obtained by F1 heterozygous intercrosses. Mice were housed in specific pathogen-free facilities. Mouse genotyping was performed by PCR using the following oligonucleotide primers:

Forward primer for wild allele: 5′-CTGCCTTCAGGAACTACATCCA CCG-3′;

Forward primer for mutant allele: 5′-TTAAGGGCCAGCTCATTCCTCC CAC-3′;

Reverse primer: 5′-ACTTCTCTGACCAGGCTTCACCAGC-3′.

### 2.3. Cell Culture

The methods for the primary culture of mouse skin fibroblasts (MSFs), mouse embryonic fibroblasts (MEFs) and bone-marrow-derived macrophages (BMDMs) were described previously (Iriyama et al., 2009; Tobiume et al., 2001).

### 2.4. Blood Chemistry

Measurements of serum TG and FFA were performed by SRL, Inc. Serum FGF21 levels were determined using an ELISA kit (R&D).

### 2.5. Histology

Tissues were fixed in 4% paraformaldehyde to make paraffin-embedded blocks. Each section (10 μm) was stained with hematoxylin and eosin.

### 2.6. Glucose and Insulin Tolerance Test

GTT was performed in 12-h-fasted mice by the intraperitoneal injection of glucose (1 g/kg B.W.). ITT was performed in 4-h-fasted mice by an intraperitoneal injection of insulin (0.75 U/kg B.W.). Blood glucose concentrations were measured with a Medi-safe mini GR-102 (TERUMO).

### 2.7. Quantification of mRNA Expression

Total RNA was isolated from tissues using the Isogen reagent (Wako) and reverse transcribed using the QuantiTect Reverse Transcription Kit (Qiagen). PCR was performed using the Power SYBR Green PCR Master Mix (Roche) and LightCycler® (Roche). All expression levels were normalized to that of S18 mRNA.

Real-time RT-PCR primers used (5′ to 3′):

| | Forward | Reverse |
|---|---|---|
| *cd36* | ttgtacctatactgtggctaaatgaga | cttgtgttttgaacatttctgctt |
| *cidea* | aaaccatgaccgaagtagcc | aggccagttgtgatgactaagac |
| *cpt1a* | gctgtcaaagataccgtgagc | tctccctccttcatcagtgg |
| *elovl3* | gaggcctctcatcctctggt | ttgccataaacttccacatcc |
| *cpt1b* | gcccatgtgctcctacca | ctctgagaggtgctgtagcaag |
| *dio2* | ctgcgctgtgtctggaac | ggagcatcttcacccagttt |
| *fgf21* | cacaccgcagtccagaaag | tgacacccaggatttgaatg |
| *lipe* (*HSL*) | agcgctggaggagtgtttt | ccgctctccagttgaacc |
| *pnpla2* (*ATGL*) | tgaccatctgccttccaga | tgtaggtggcgcaagaca |
| *slc27a1* (*FATP1*) | gacaagctggatcaggcaag | gaggccacagaggctgttc |
| *slc27a3* (*FATP3*) | gagaacttgccaccgtatgc | ggtctcagtagtggccaaaga |
| *slc27a4* (*FATP4*) | ggcagtgagatggcctca | cagagcagaagaggctgagtg |
| *S18* | tccagcacattttgcgagta | cagtgatggcgaaggctatt |
| *ucp1* | gatgtggtaaaaacaagattcatca | cgcagaaaagaagccacaa |

### 2.8. Immunoblot Analysis

Tissues were lysed with IP lysis buffer (20 mM Tris–HCl, pH 7.5, 150 mM NaCl, 10 mM EDTA, pH 7.5, 1% Na-deoxycholate, 1% Triton X-100) with protease inhibitors (1 mM phenylmethylsulfonyl fluoride, 5 mg/mL leupeptin) and a 25× phosphatase inhibitor cocktail (200 mM NaF, 300 mM beta-glycerophosphate, 25 mM $Na_3VO_4$, 30 mM $Na_2MoO_4$, 50 mM Imidazole). The lysates were resolved by SDS-PAGE and electroblotted onto polyvinylidene difluoride membranes. After blocking with 5% skim milk in TBS-T (50 mM Tris–HCl, pH 8.0,

150 mM NaCl and 0.05% Tween 20), the membranes were probed with antibodies. The antibody/antigen complexes were detected using the ECL system (GE Healthcare).

### 2.9. The Measurement of VLDL Release From Liver

Fasted mice were intravenously injected with 100 μl/20 g body weight 10% Triton WR-1339 (Santa Cruz) in PBS and subsequently exposed to cold. After 4 h, serum was collected, and TG measurements were performed by SRL, Inc.

### 2.10. The ISRIB Treatment

Fasted mice were intraperitoneally injected with 2.5 mg/kg body weight ISRIB (Sigma) in buffer (12.5% DMSO, 12.5% PEG400, 75% PBS) and subsequently exposed to cold. After 5 h, BAT was dissected and subjected to subsequent analyses.

### 2.11. Indirect Calorimetry

Whole-body $O_2$ consumption was measured using an open-circuit four-chamber indirect calorimetry system (Muromachi). Mice had *ad libitum* access to food and water, and data were recorded for a 24-h period with light from 7:00 to 19:00.

### 2.12. Electron Microscopic Analysis

For electron microscopy, the brown adipose tissues were quickly removed from the mice that had been deeply anesthetized and fixed by cardiac perfusion with 2% paraformaldehyde-2% glutaraldehyde buffered with 0.1 mol/L phosphate buffer, were post-fixed with 2% $OsO_4$, dehydrated with a graded series of alcohol, and embedded in Epon 812. Ultrathin sections were cut with an ultramicrotome (UC6; Leica Microsystems, Vienna, Austria), stained with uranyl acetate and lead citrate, and observed with a Hitachi HT7700 electron microscope (Hitachi, Tokyo, Japan). The mean gray scale value of each mitochondrion was measured using Image J. Approximately 150 mitochondria from 8–9 images for each mouse and approximately 450 mitochondria in total for each genotype were analyzed ($n = 3$).

### 2.13. Antibodies

For immunoblot analysis, the following primary antibodies were used: α-tubulin (Santa Cruz), UCP1 (Abcam), FGF21 (Santa Cruz), phospho-eif2α (Cell Signaling) and eif2α (Santa Cruz). The generation of the rabbit polyclonal anti-PGAM5 antibody (RTL) was described previously (Takeda et al., 2009).

## 3. Results

### 3.1. Pgam5 Knockout (KO) Mice Exhibit a Resistance Phenotype Against Cold Stress Under Fasting Condition

To address the *in vivo* functions of PGAM5 in mammals, we engineered a targeting vector to generate whole-body Pgam5 knockout (KO) mice (Figure S1a). Homozygosity for the mutation was confirmed by Southern blot and PCR analyses (Figure S1b), and a complete ablation of PGAM5 protein was also confirmed by immunoblot analysis using several primary cell lines that were derived from the generated Pgam5 KO mice (Figure S1c). Pgam5 KO mice were viable and developed normally with no obvious phenotypes, at least during the early stage of life.

Previous studies by us and others have speculated that PGAM5 is a mitochondria-resident stress-responsive molecule (Chen et al., 2014; Lu et al., 2014; Sekine et al., 2012; Wang et al., 2012; Zhuang et al., 2013). Hence, we examined the phenotypes of Pgam5 KO mice under cold exposure as one of the *in vivo* models that might impose stresses on mitochondria *in vivo*. We tested a metabolically severe cold-stress model. In this model, mice are first kept under fasted conditions and are subsequently subjected to cold exposure (Fig. 1a, left panel). As a result, we found that the ablation of Pgam5 dramatically protects mice against cold stress when combined with fasting. The survival rate of Pgam5 KO mice was significantly prolonged compared with that of WT mice (Fig. 1a, right panel), and Pgam5 KO mice maintained their core body temperature even after a 6-h cold exposure under fasting conditions (Fig. 1b). Interestingly, Pgam5 KO mice showed similar vulnerability as WT mice when separately exposed to either cold stress (Fig. 1c) or fasting (Fig. 1d and e), indicating that fasting is required for the resistance of Pgam5 KO mice to cold stress.

### 3.2. The Ablation of Pgam5 Affects Lipid Metabolism Under Fasting and Cold Stress

As mentioned above, UCP1, as an uncoupler of mitochondrial respiration, plays crucial roles in adaptive thermogenesis in BAT (Krauss et al., 2005). Therefore, we next examined the mRNA expression of *Ucp1* in BAT derived from Pgam5 KO mice under fasting and cold stress. Although the mRNA expression of the *Ucp1* gene slightly increased (Figure S2a), the protein expression level of UCP1 in Pgam5-deficient BAT was similar to that in WT mice (Figure S2b). mRNA expressions of other thermogenesis-related genes were also comparable between WT and Pgam5 KO mice (Figure S2a). Thus, we next focused on lipid metabolism, another important factor for cold resistance (Townsend and Tseng, 2014). We found that the triglyceride (TG) level in serum was significantly reduced in Pgam5 KO mice under fasting and cold stress (Fig. 2a, left panel), although obvious differences were not observed in the serum FFA level (Fig. 2a, right panel). The serum TG level of Pgam5 KO mice was comparable to that of WT mice upon pre-treatment with triton WR-1339 (Fig. 2b), which blocks TG removal from plasma by inhibiting lipoprotein lipase (LPL) and is thus often used to estimate the rate of TG entry into the plasma from the liver (Goudriaan et al., 2005). Therefore, it is likely that the reduced TG level in the serum of Pgam5 KO mice is not due to decreased TG release from the liver but results from enhanced TG uptake and utilization in certain tissues.

It is reported that cold exposure accelerates the plasma clearance of TG as a result of increased TG uptake and utilization in activated BAT (Bartelt et al., 2011). Indeed, a significant reduction of the BAT weight ratio was observed in Pgam5 KO mice under the fasting and cold stress-condition (Fig. 2c and d). Although the difference was not statistically significant, the slight decrease of BAT weight ratio was also observed in Pgam5-deficient mice from steady state (Fig. 2d). Actually, H&E staining of BAT sections revealed that the lipid content of BAT in Pgam5 KO mice decreased from the basal level (Fig. 2e). Moreover, the decrease of lipid content in Pgam5-deficient BAT became more evident after fasting and cold stress compared with that in WT mice-derived BAT (Fig. 2f). By contrast, no significant weight loss was observed in other tissues derived from Pgam5 KO mice, such as the inguinal white adipose tissue (iWAT), epididymal white adipose tissue (eWAT) and liver (Fig. 2g). These results suggest that the ablation of Pgam5 affects lipid metabolism, most significantly in BAT, under fasting and cold stress.

We next examined the expression amount of lipid metabolism-related genes focusing on BAT. mRNA expressions of most genes related to lipid transport, lipolysis, and β-oxidation in BAT of Pgam5 KO mice were comparable to those of WT mice either under basal or fasting and cold stress-loaded conditions (Figure S3a, b and c). However, we found that the mRNA expression of *Elovl3* was significantly enhanced in Pgam5 KO-mice-derived BAT (Fig. 2e). ELOVL3 belongs to the ELOVL family of proteins that act to elongate FFAs into very long chain fatty acids (VLCFAs) (Westerberg et al., 2006). *Elovl3* expression is reported to be induced after cold exposure, and Elovl3-deficient mice are only able to survive the cold by shivering because they lack the elongation activity of FFAs that is needed for thermogenesis in BAT (Westerberg et al., 2006). Taken all together, it would be possible that the enhancement of *Elovl3* expression in Pgam5-deficient BAT is one of the causal factors promoting lipid utilization in BAT and conferring subsequent cold resistance to Pgam5 KO mice.

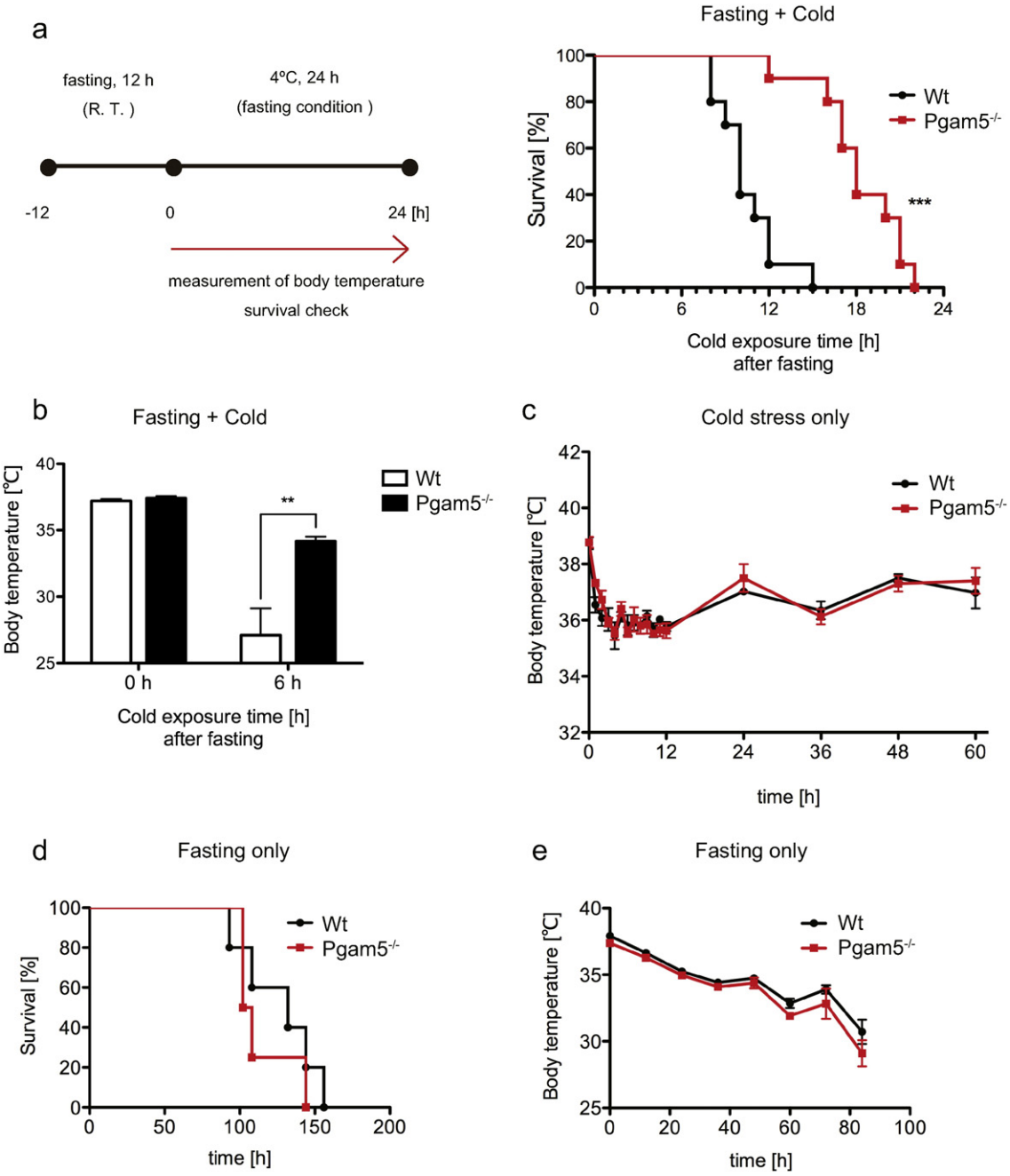


**Fig. 1.** Pgam5 knockout (KO) mice exhibit a resistance phenotype against cold stress under fasting condition. (a, b) Survival rate and body temperature of WT and Pgam5 KO mice at the indicated time periods after cold exposure combined with fasting (n = 10). (c) The body temperatures of cold-exposed WT and Pgam5 KO mice were monitored for 60 h under fed conditions (n = 4). (d, e) The survival rate (d) and body temperatures (e) of WT and Pgam5 KO mice were monitored at the indicated time periods under fasting conditions (WT; n = 6, KO; n = 5). Data are expressed as the means ± SEM, $^{**}p < 0.01$, $^{***}p < 0.001$; log rank test (a), unpaired Student's t-test (b).

### *3.3. Pgam5-deficient BAT Exhibits Altered Mitochondrial Integrity Under Fasting and Cold Stress*

Because PGAM5 is a mitochondria-resident protein, we next examined the mitochondrial integrity in BAT under fasting and cold stress. Although there were no striking differences in mitochondrial morphology under basal conditions (Fig. 3a), electron microscopy analysis revealed that electron-dense mitochondria appear in Pgam5-deficient BAT under fasting and cold stress (Fig. 3b and c). Quantitative evaluation of electron density of each mitochondrion revealed that the number of electron-dense mitochondria increased in Pgam5-deficient BAT under fasting and cold stress (Fig. 3d and e).

Similar electron-dense mitochondria were reported to be observed in induced pluripotent stem cells (iPSCs) from Parkinson's disease patients harboring causative gene mutations in the *Parkin* gene (Imaizumi et al., 2012). Because recent studies have suggested that Parkin deficiency results in the accumulation of dysfunctional mitochondria due to impaired autophagic degradation of damaged mitochondria (Youle and Narendra, 2011), the electron-dense abnormal mitochondria observed in iPSCs from Parkinson's disease patients were thought to be dysfunctional. Thus, the electron-dense mitochondria in Pgam5-deficient BAT under fasting and cold stress could also be interpreted as dysfunctional mitochondria. These results suggest that Pgam5 deficiency results in the failure of preservation of proper

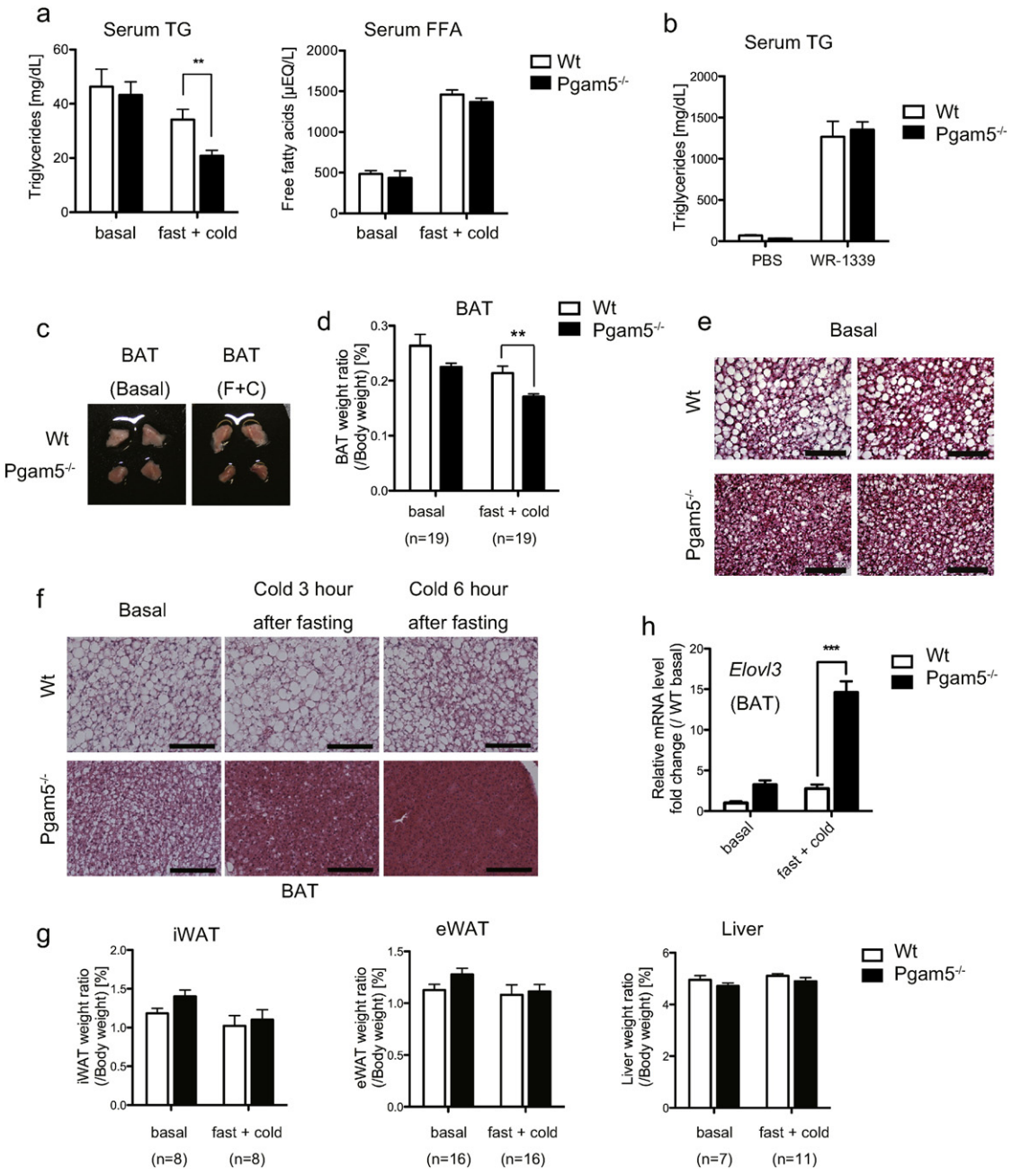


**Fig. 2.** The ablation of Pgam5 affects lipid metabolism under fasting and cold stress. (a) The triglyceride (TG) and free fatty acid (FFA) levels in the serum of WT and Pgam5 KO mice under a 6-h cold exposure after 12 h of fasting (n = 21). (b) Estimation of TG release from liver using a lipoprotein lipase (LPL) inhibitor, Triton WR-1339. After 12 h of fasting, WT and Pgam5 KO mice were intravenously treated with PBS or Triton WR-1339 and subjected to cold stress. After 4 h of cold exposure, the serum TG level was measured (n = 8). (c) Representative gross image of BAT from WT and Pgam5 KO mice under basal conditions or at 5 h of cold exposure after 12 h of fasting. (d) BAT weight ratio of WT and Pgam5 KO mice at 6-h cold exposure after 12-h of fasting. (e and f) Representative H&E staining of BAT sections from WT and Pgam5 KO mice under the indicated conditions. Scale bars, 100 μm. (g) Several-tissue weight ratio of WT and Pgam5 KO mice at 6 h of cold exposure after 12 h of fasting. (h) Expression of *Elovl3*, an elongation factor of FFAs in BAT from WT and Pgam5 KO mice under basal conditions or at 6 h of cold exposure after 12 h of fasting was determined *via* quantitative RT-PCR (n = 4). Data are expressed as the mean ± SEM, $^{**}p < 0.01$, $^{***}p < 0.001$; unpaired Student's t-test (a and d), two-way ANOVA/Bonferroni post-test (g). BAT, brown adipose tissue; iWAT, inguinal white adipose tissue; eWAT, epididymal white adipose tissue.

mitochondrial integrity under fasting and cold stress, one of the stress conditions that may impose metabolic challenges on mitochondria.

### *3.4. FGF21 Expression is Enhanced in Pgam5-deficient BAT Under Fasting and Cold Stress*

Although the proper mitochondrial integrity was reduced in BAT, an important tissue for adaptive thermogenesis (Fig. 3b–e), Pgam5 KO mice were resistant against fasting and cold stress (Fig. 1a and b). Thus, we hypothesized that some compensatory mechanisms may operate in Pgam5-deficient BAT in order to maintain the whole-body homeostasis.

Fibroblast growth factor 21 (FGF21) is known to be induced in response to several stresses, including fasting and cold stress, and ultimately confers resistance to these metabolic stresses by promoting fuel delivery (Badman et al., 2009; Potthoff et al., 2009) and adaptive thermogenesis (Fisher et al., 2012; Hondares et al., 2010). Moreover, several recent reports suggested that dysfunctional mitochondria induce FGF21 (Dogan et al., 2014; Keipert et al., 2014; Kim et al., 2013a,b). Strikingly, we found that mRNA expression of *Fgf21* was greatly enhanced in Pgam5-deficient BAT (Fig. 4a). Because it is known that FGF21 is released from various tissues, including BAT, liver and muscle, depending on the type of stress (Owen et al., 2015), we next examined the tissue specificity

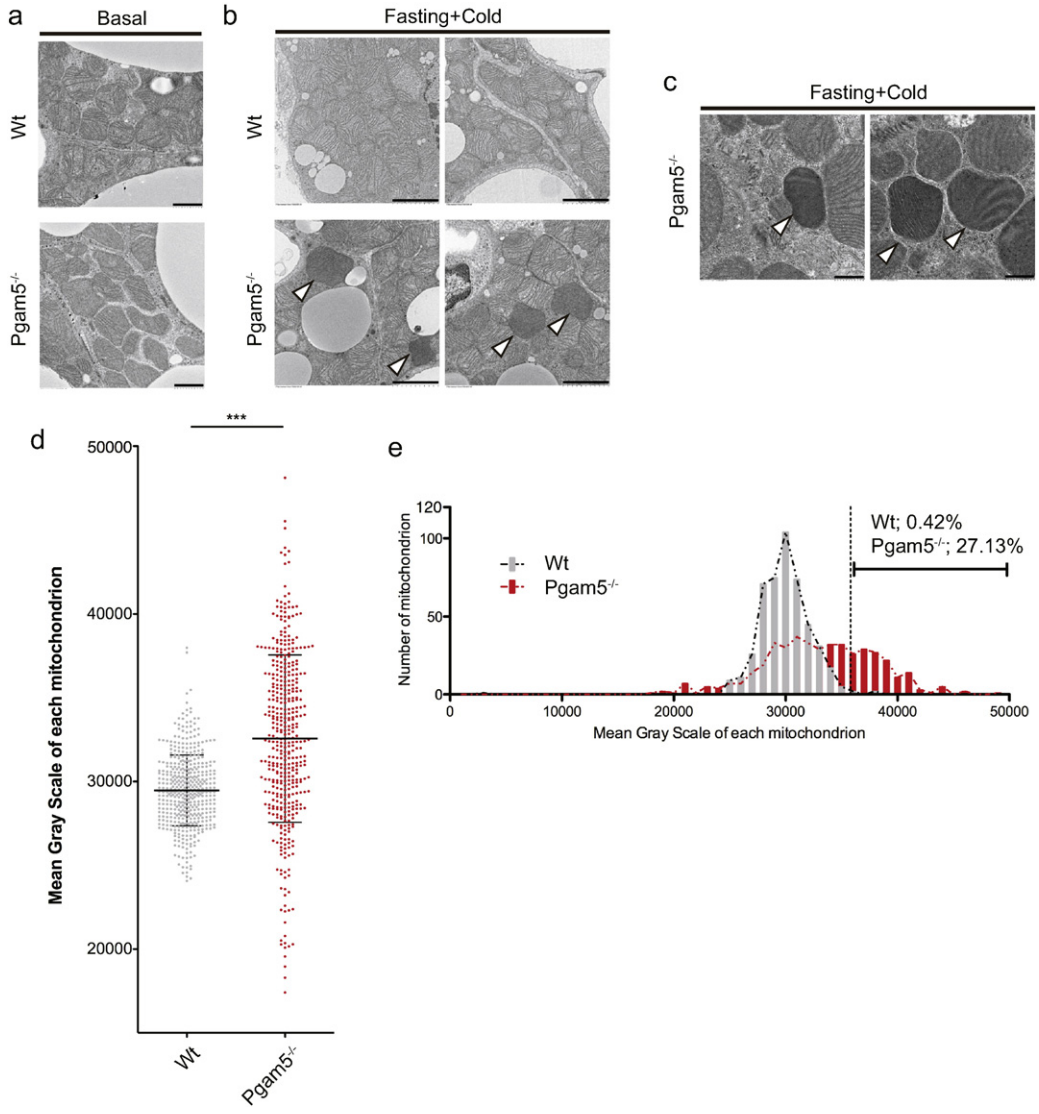


**Fig. 3.** Pgam5-deficient BAT exhibits altered mitochondrial integrity under fasting and cold stress. (a, b and c) Representative electron micrographs of mitochondria in BAT derived from WT and Pgam5 KO mice under basal conditions (a) or at 6 h of cold exposure after 12 h of fasting (b and c). Images in (b) and (c) were obtained from different experiments. Scale bars, 1.0 μm (a), 2.0 μm (b) and 500 nm (c). White arrowheads indicate electron-dense mitochondria. (d and e) The quantitative evaluation of electron density of each mitochondrion in (b). The mean gray scale value was measured using Image J for each mitochondrion in BAT derived from WT and Pgam5 KO mice. Approximately 150 mitochondria from 8–9 images for each mouse and approximately 450 mitochondria in total for each genotype were analyzed ($n = 3$). Data are means ± SD, $^{***}p < 0.001$; unpaired Student's t-test (d). Mitochondria whose mean gray scale value was greater than the Average + 3SD of WT mice were designated as electron-dense mitochondria, and their relative frequency was calculated (e).

and stress dependence of the enhancement of *Fgf21* in Pgam5-deficient BAT. In addition to BAT, the expression level of *Fgf21* mRNA was slightly but significantly enhanced in Pgam5 KO mice-derived iWAT, but not in other tissues such as liver and muscle (Fig. 4b).

Moreover, the enhancement of *Fgf21* in Pgam5-deficient BAT was only observed under fasting and cold together but not under fasting or cold stress alone (Fig. 4c), which correlates with the phenotypes for body temperature and survival (Fig. 1a-e). Immunoblot analysis using BAT lysates derived from mice that were treated with fasting and cold stress revealed that the enhancement of FGF21 also occurs at the protein level in Pgam5 KO mice (Fig. 4d). These results suggest that the ablation of Pgam5 promotes *Fgf21* gene expression in a tissue- and stress-specific manner.

### *3.5. The Enhancement of FGF21 in Pgam5-deficient BAT is Induced by the Phospho-eif2α-ATF4 Pathway*

We next attempted to identify the signaling pathway that regulates FGF21 induction in Pgam5-deficient BAT under fasting and cold stress. The phosphorylation of eif2α is induced by several stresses and subsequently triggers several gene expression programs by enhancing the translation of transcription factors, including ATF4, which is called the integrated stress response (ISR) (Baird and Wek, 2012). In addition, it has recently been reported that mitochondrial dysfunction due to the deficiency of the autophagy-dependent clearance of damaged mitochondria can also activate the phospho-eif2α-ATF4 pathway, which results in FGF21 induction (Kim et al., 2013b). Interestingly, the phosphorylation of eif2α in Pgam5-deficient BAT is markedly enhanced under fasting and cold stress compared with that observed in WT mice (Fig. 4d). Moreover, the pre-treatment with ISRIB, a recently identified phospho-eif2α-ATF4 pathway-selective inhibitor (Sekine et al., 2015; Sidrauski et al., 2013), almost completely suppressed the enhancement of *Fgf21* induction in Pgam5-deficient BAT under fasting and cold stress (Fig. 4e). These results suggest that the ablation of Pgam5 fails to maintain proper mitochondrial integrity under fasting and cold stress, which might ultimately lead to phospho-eif2α-ATF4-pathway-dependent FGF21 induction.

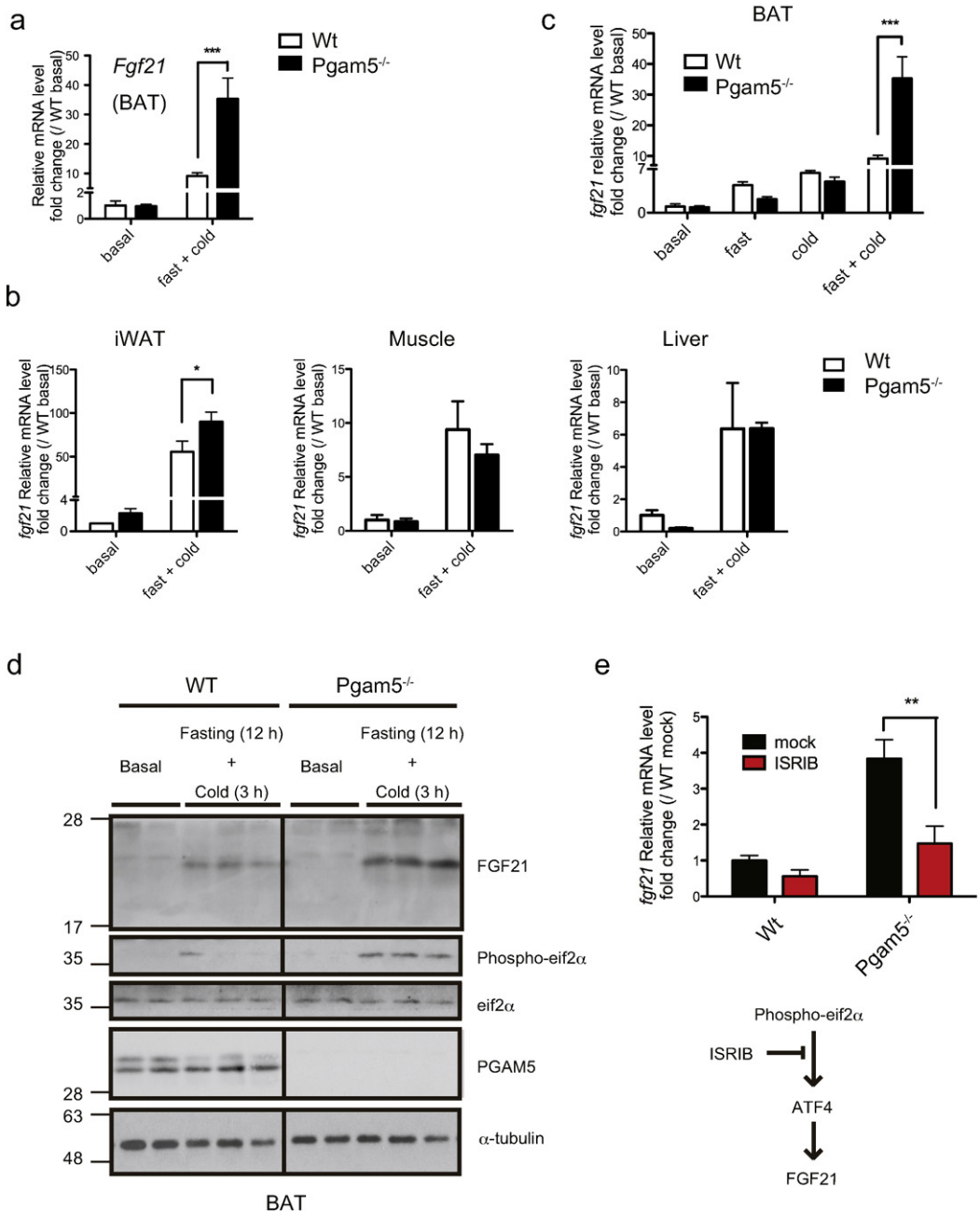


**Fig. 4.** Phospho-eif2α-ATF4-pathway-mediated FGF21 induction is enhanced in Pgam5 KO-mice-derived brown adipose tissue under fasting and cold stress. (a and b) *Fgf21* gene expression in the indicated tissues from WT and Pgam5 KO mice under basal conditions or at 6 h of cold exposure after 12 h of fasting according to quantitative RT-PCR (n = 4). (c) *Fgf21* gene expression in BAT derived from WT and Pgam5 KO mice under basal conditions, 18 h after fasting only (fast), 6 h after cold stress only (cold), and 6 h of cold exposure after 12 h of fasting (fast + cold) was determined using quantitative RT-PCR (n = 4). (d) Representative immunoblots for the indicated proteins derived from WT and Pgam5 KO mice under basal conditions or at 3 h of cold exposure after 12 h of fasting. (e) After fasting for 12 h, WT and Pgam5 KO mice were treated with 2.5 mg/kg body weight ISRIB or mock i.p. and subsequently exposed to cold stress. After 5 h, *Fgf21* gene expression in BAT was determined using quantitative RT-PCR (WT; n = 4 for each, Pgam5 KO; mock n = 3, ISRIB n = 4). Data are expressed as the mean ± SEM, *p < 0.05, **p < 0.01, ***p < 0.001; two-way ANOVA/Bonferroni post-test (a, b, c, and e). BAT, brown adipose tissue; iWAT, inguinal white adipose tissue; CNS, central nervous systems.

### *3.6. Pgam5 KO Mice Show Lean Phenotypes Against a High-fat-diet-induced Obesity Model*

Finally, because cold sensitivity and resistance phenotypes in mice are well correlated with obese and lean phenotypes, respectively (Lin and Li, 2004), we examined the impact of metabolic stress by feeding Pgam5 KO mice a high-fat diet (HFD). The weight gain in HFD-fed Pgam5 KO mice was dramatically suppressed compared with that in WT mice (Fig. 5a and b). Although there were no obvious differences in fat mass or liver mass between WT mice and Pgam5 KO mice under chow diet (CD)-fed conditions (Fig. 5c), a significant reduction of the fat mass and liver mass in HFD-fed Pgam5 KO mice was observed compared with WT mice (Fig. 5d and e). H&E staining of BAT and iWAT also supports the suppression of lipid accumulation in HFD-fed Pgam5 KO mice (Fig. 5f).

In addition to decreased fat mass, an intraperitoneal glucose tolerance test (GTT) and insulin tolerance test (ITT) revealed that Pgam5 KO mice had enhanced glucose tolerance and insulin sensitivity compared with WT mice (Fig. 5g and h). Moreover, although whole-body energy expenditure in Pgam5 KO mice was comparable to that of WT mice under CD-fed conditions (Fig. 5i), energy expenditure was significantly enhanced compared with that of WT mice under HFD-fed

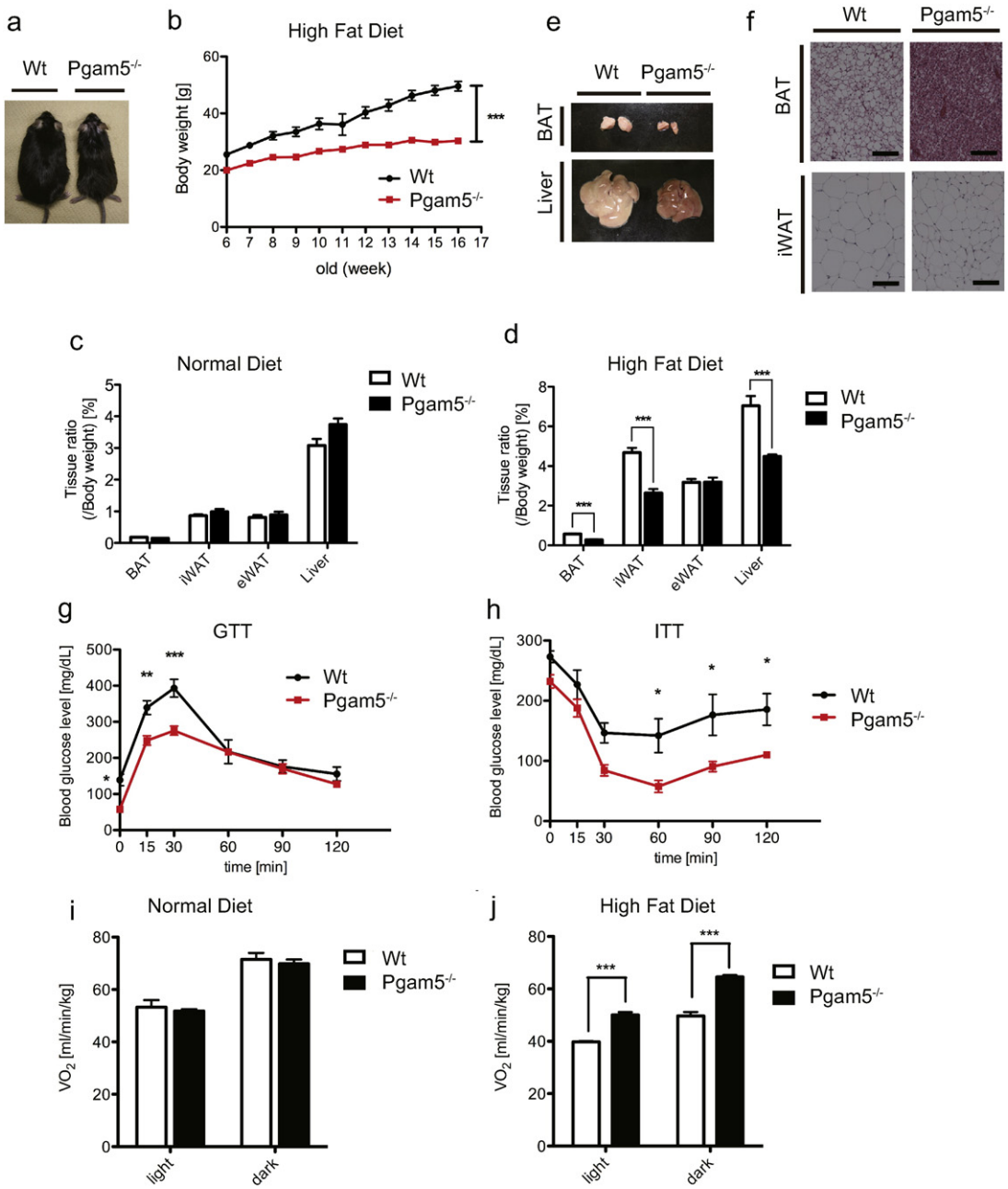


**Fig. 5.** Pgam5 KO mice are resistant to high-fat-diet-induced obesity. (a) Representative picture of 16-week-old mice that were fed a high-fat diet (HFD) for 11 weeks. (b) Body weights of WT and Pgam5 KO mice that were fed a HFD (n = 5). (c and d) Tissue weight ratio-normalized body weights of WT and Pgam5 KO mice under CD (n = 4) (c) or HFD for 12 weeks (n = 8) (d). (e) Representative gross image of BAT and liver from WT and Pgam5 KO mice that were fed a HFD for 12 weeks. (f) Representative H&E staining of the indicated fat sections from WT and Pgam5 KO mice that were fed a HFD for 7 weeks. Scale bars, 100 μm. (g and h) GTT (g) in WT and Pgam5 KO mice that were fed a HFD for 12 weeks (n = 5) and ITT (h) in WT and Pgam5 KO mice that were fed a HFD for 8 weeks (n = 6). (i and j) Oxygen consumption of male 9-week-old WT and Pgam5 KO mice under CD (n = 4) (i) and 16-week-old WT and Pgam5 KO mice that were fed a HFD for 12 weeks (n = 4) (j). Data are expressed as the mean ± SEM, $^{*}p < 0.05$, $^{**}p < 0.01$, $^{***}p < 0.001$; unpaired Student's t-test (c, d, i and j), two-way ANOVA/Bonferroni post-test (b, g, and h). BAT, brown adipose tissue; iWAT, inguinal white adipose tissue; eWAT, epididymal white adipose tissue.

conditions (Fig. 5j). These results indicate that the ablation of Pgam5 protects mice from HFD-induced obesity.

## 4. Discussion

In this report, we uncovered two metabolic-stress-related phenotypes of Pgam5 KO mice. In our analysis of the cold-resistance phenotypes of Pgam5 KO mice under fasting condition, we focused especially on BAT, a center of adaptive thermogenesis. Under cold exposure, it is known that BAT is a major tissue that takes up TGs from the blood stream (Bartelt et al., 2011). In BAT, TGs that were transported from the blood stream and those that were stored in lipid droplets were degraded to release FFAs *via* lipolysis in response to cold (Townsend and Tseng, 2014). The released FFAs not only become fuel for β-oxidation but also promote adaptive thermogenesis through activating UCP1-mediated thermogenesis (Fedorenko et al., 2012). Thus, the enhanced lipid utilization in BAT is critical for cold resistance. Of note, several signs of enhanced lipid metabolism were observed in Pgam5 KO mice after fasting and cold stress: serum TGs decreased in Pgam5 KO mice (Fig. 2a), lipid droplets were significantly smaller in Pgam5-deficient BAT (Fig. 2f), and the expression level of lipid elongation factor, *Elovl3* was enhanced in Pgam5-deficient BAT (Fig. 2h). These observations

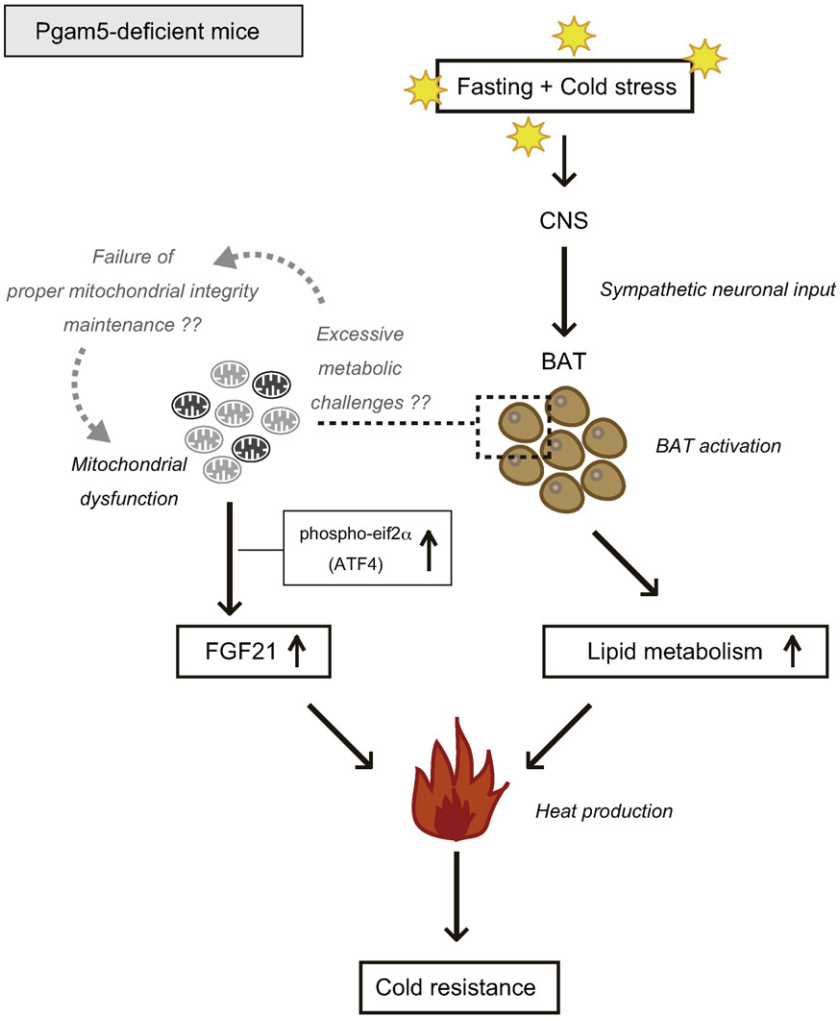


**Fig. 6.** Summary of phenotypes of Pgam5 KO mice under the fasting and cold stress. See detailed explanation in Discussion.

suggest that the ablation of Pgam5 results in the enhancement of lipid uptake and utilization in BAT, which ultimately confers the cold resistance to mice (Fig. 6). Because the decrease of lipid content in Pgam5-deficient BAT was striking (Fig. 2e and f), uncovering the precise mechanisms by which mitochondria-resident PGAM5 regulates the activity of BAT is expected in the future study. Interestingly, recent report suggests that adrenergic stimulation promotes rapid mitochondrial fission in brown adipocytes, which ultimately results in promoting energy expenditure (Wikstrom et al., 2014). Moreover, it has been reported that the ablation PGAM5 promotes rapid mitochondrial fragmentation in some cells under several stress conditions (Wang et al., 2012; Moriwaki et al., 2016). Thus, it would be possible that PGAM5 in BAT might be also involved in the regulation of mitochondrial dynamics. Alternatively, considering that the lipid metabolism in BAT is known to be activated by sympathetic nervous system, it would be possible that the enhanced lipid metabolism observed in Pgam5-deficient BAT is induced by the increased sympathetic neuronal input. For further understanding of the roles of PGAM5 in lipid metabolism in BAT, it is required to determine in which tissues PGAM5 exert its roles, *i.e.* in BAT itself, central nervous system, or even other tissues.

Another critical alteration in Pgam5-deficient BAT under fasting and cold stress is the enhancement of FGF21 (Fig. 4a and d). Because the pre-treatment of ISRIB almost completely blocked the enhancement of *Fgf21* expression in Pgam5-deficient BAT (Fig. 4e), phospho-eif2α-ATF4 pathway may be involved in the enhanced FGF21 induction. From the previous analysis of Fgf21 KO mice, it is known that FGF21 contributes to cold resistance (Fisher et al., 2012). In addition, FGF21 has been shown to promote lipid metabolism (Owen et al., 2015). Unexpectedly, however, the pre-treatment of ISRIB did not suppress the enhanced lipid metabolism observed in Pgam5 KO mice (Figure S4a and b). Therefore, FGF21 induction may not be causal for the enhancement of lipid metabolism at least in Pgam5 KO mice (Fig. 6).

Several recent reports suggested that dysfunctional mitochondria activate the phospho-eif2α-ATF4 pathway, which eventually leads to FGF21 induction (Dogan et al., 2014; Keipert et al., 2014; Kim et al., 2013a,b). Enhanced eif2α phosphorylation (Fig. 4d) and electron-dense abnormal mitochondria (Fig. 3b-e) were observed in Pgam5-deficient BAT after fasting and cold stress. From these observations, we now hypothesize that the appearance of dysfunctional mitochondria in Pgam5-deficient BAT under fasting and cold stress might activate the phospho-eif2α-ATF4 pathway, which triggers the FGF21 induction (Fig. 6). Uncovering the precise molecular mechanisms by which PGAM5 protects proper mitochondrial integrity under fasting and cold stress is one of the most tempting future directions. It would be possible that PGAM5 in BAT itself protects proper mitochondrial integrity from metabolic perturbations. Alternatively, it could be speculated that exhausted mitochondria intolerable to metabolic challenges caused by the enhanced lipid metabolism may give rise to dysfunctional mitochondria in Pgam5-deficient BAT.

The resistance to HFD-induced obesity was another drastic phenotype of Pgam5 KO mice (Fig. 5a–j). It has been reported that the administration of FGF21 or its analogs induces weight loss through increased energy expenditure (Coskun et al., 2008; Gaich et al., 2013; Kharitonenkov et al., 2005). Because FGF21 induction was enhanced in

Pgam5-deficient BAT under fasting and cold stress (Fig. 4a, c and d), we examined the possibility that its enhancement also contributes to the lean phenotype of Pgam5 KO mice under HFD-fed conditions. However, serum FGF21 concentration was even reduced in Pgam5 KO mice under HFD-fed conditions (Figure S5). Several previous studies also reported that the serum FGF21 level is rather increased in obese animals compared with lean animals (Zhang et al., 2008), raising the possibility that obesity is an FGF21-resistance condition (Fisher et al., 2010). Thus, the above results in Pgam5 KO mice might reflect these previous observations. The identification of the factors that are responsible for the resistance of Pgam5 KO mice to HFD-induced obesity is expected in future studies. Several clinical studies suggest the inverse correlation between the BAT activity and body fatness (Lee et al., 2014). In this aspect, it is noteworthy that the lipid utilization might be activated in Pgam5-deficient BAT under stressed conditions or even from basal state (Fig. 2f and e). Moreover, very recently, it has been reported that PGAM5 KO mice show slight decrease of body weight from basal state (Moriwaki et al., 2016). The elucidation of the mechanisms of enhanced lipid metabolism in Pgam5-deficient BAT may not only uncover the reasons why Pgam5 KO mice show such a drastic lean phenotype but also provide some clinical clues to the therapeutic targets for human obesity and related metabolic disorders.

In this report, we found that mitochondria-resident stress responsive protein PGAM5 acts as a metabolic regulator *in vivo*. We hope that our study will provide a key to uncover more detailed functions of PGAM5 as a metabolic regulator and will shed new light on mitochondrial stress-responsive molecules as potential therapeutic targets for metabolic disorders.

## Conflicts of Interest

The authors declare that they have no conflicts of interest.

## Author Contributions

S. Sekine and A.Y. conducted almost all the experiments. M.K. and Y.U. conducted electron microscopy analysis. S. Sekine, A.Y. and H. I. designed experiments and wrote the paper. K.H., S. Sugawara, I.N. and K.T. supported this work. K.T. also contributed to the generation of Pgam5 KO mice.

## Acknowledgments

This work was supported by a Grant-in-Aid for Scientific Research (KAKENHI) from the Japan Society for the Promotion of Science (JSPS) and the Japanese Ministry of Education, Culture, Sports, Science and Technology (MEXT) (Grant number; 25221302 to H. Ichijo), and Ono Medical Research Foundation (to H. Ichijo).

## Appendix A. Supplementary Data

Supplementary data to this article can be found online at http://dx.doi.org/10.1016/j.ebiom.2016.01.031.

## References

Badman, M.K., Koester, A., Flier, J.S., Kharitonenkov, A., Maratos-Flier, E., 2009. Fibroblast growth factor 21-deficient mice demonstrate impaired adaptation to ketosis. Endocrinology 150, 4931–4940.

Baird, T.D., Wek, R.C., 2012. Eukaryotic initiation factor 2 phosphorylation and translational control in metabolism. Adv. Nutr. 3, 307–321.

Bartelt, A., Bruns, O.T., Reimer, R., Hohenberg, H., Ittrich, H., Peldschus, K., Kaul, M.G., Tromsdorf, U.I., Weller, H., Waurisch, C., et al., 2011. Brown adipose tissue activity controls triglyceride clearance. Nat. Med. 17, 200–205.

Chartoumpekis, D.V., Habeos, I.G., Ziros, P.G., Psyrogiannis, A.I., Kyriazopoulou, V.E., Papavassiliou, A.G., 2011. Brown adipose tissue responds to cold and adrenergic stimulation by induction of FGF21. Mol. Med. 17, 736–740.

Chen, G., Han, Z., Feng, D., Chen, Y., Chen, L., Wu, H., Huang, L., Zhou, C., Cai, X., Fu, C., et al., 2014. A regulatory signaling loop comprising the PGAM5 phosphatase and CK2 controls receptor-mediated mitophagy. Mol. Cell 54, 362–377.

Coskun, T., Bina, H.A., Schneider, M.A., Dunbar, J.D., Hu, C.C., Chen, Y., Moller, D.E., Kharitonenkov, A., 2008. Fibroblast growth factor 21 corrects obesity in mice. Endocrinology 149, 6018–6027.

Dogan, S.A., Pujol, C., Maiti, P., Kukat, A., Wang, S., Hermans, S., Senft, K., Wibom, R., Rugarli, E.I., Trifunovic, A., 2014. Tissue-specific loss of DARS2 activates stress responses independently of respiratory chain deficiency in the heart. Cell Metab. 19, 458–469.

Ellis, J.M., Li, L.O., Wu, P.C., Koves, T.R., Ilkayeva, O., Stevens, R.D., Watkins, S.M., Muoio, D.M., Coleman, R.A., 2010. Adipose acyl-CoA synthetase-1 directs fatty acids toward beta-oxidation and is required for cold thermogenesis. Cell Metab. 12, 53–64.

Enerback, S., Jacobsson, A., Simpson, E.M., Guerra, C., Yamashita, H., Harper, M.E., Kozak, L.P., 1997. Mice lacking mitochondrial uncoupling protein are cold-sensitive but not obese. Nature 387, 90–94.

Fedorenko, A., Lishko, P.V., Kirichok, Y., 2012. Mechanism of fatty-acid-dependent UCP1 uncoupling in brown fat mitochondria. Cell 151, 400–413.

Fisher, F.M., Chui, P.C., Antonellis, P.J., Bina, H.A., Kharitonenkov, A., Flier, J.S., Maratos-Flier, E., 2010. Obesity is a fibroblast growth factor 21 (FGF21)-resistant state. Diabetes 59, 2781–2789.

Fisher, F.M., Kleiner, S., Douris, N., Fox, E.C., Mepani, R.J., Verdeguer, F., Wu, J., Kharitonenkov, A., Flier, J.S., Maratos-Flier, E., et al., 2012. FGF21 regulates PGC-1alpha and browning of white adipose tissues in adaptive thermogenesis. Genes Dev. 26, 271–281.

Gaich, G., Chien, J.Y., Fu, H., Glass, L.C., Deeg, M.A., Holland, W.L., Kharitonenkov, A., Bumol, T., Schilske, H.K., Moller, D.E., 2013. The effects of LY2405319, an FGF21 analog, in obese human subjects with type 2 diabetes. Cell Metab. 18, 333–340.

Goudriaan, J.R., den Boer, M.A., Rensen, P.C., Febbraio, M., Kuipers, F., Romijn, J.A., Havekes, L.M., Voshol, P.J., 2005. CD36 deficiency in mice impairs lipoprotein lipase-mediated triglyceride clearance. J. Lipid Res. 46, 2175–2181.

Hondares, E., Rosell, M., Gonzalez, F.J., Giralt, M., Iglesias, R., Villarroya, F., 2010. Hepatic FGF21 expression is induced at birth via PPARalpha in response to milk intake and contributes to thermogenic activation of neonatal brown fat. Cell Metab. 11, 206–212.

Hondares, E., Iglesias, R., Giralt, A., Gonzalez, F.J., Giralt, M., Mampel, T., Villarroya, F., 2011. Thermogenic activation induces FGF21 expression and release in brown adipose tissue. J. Biol. Chem. 286, 12983–12990.

Imaizumi, Y., Okada, Y., Akamatsu, W., Koike, M., Kuzumaki, N., Hayakawa, H., Nihira, T., Kobayashi, T., Ohyama, M., Sato, S., et al., 2012. Mitochondrial dysfunction associated with increased oxidative stress and alpha-synuclein accumulation in PARK2 iPSC-derived neurons and postmortem brain tissue. Mol. Brain 5, 35.

Iriyama, T., Takeda, K., Nakamura, H., Morimoto, Y., Kuroiwa, T., Mizukami, J., Umeda, T., Noguchi, T., Naguro, I., Nishitoh, H., et al., 2009. ASK1 and ASK2 differentially regulate the counteracting roles of apoptosis and inflammation in tumorigenesis. EMBO J. 28, 843–853.

Jedrzejas, M.J., 2000. Structure, function, and evolution of phosphoglycerate mutases: comparison with fructose-2,6-bisphosphatase, acid phosphatase, and alkaline phosphatase. Prog. Biophys. Mol. Biol. 73, 263–287.

Ji, S., You, Y., Kerner, J., Hoppel, C.L., Schoeb, T.R., Chick, W.S., Hamm, D.A., Sharer, J.D., Wood, P.A., 2008. Homozygous carnitine palmitoyltransferase 1b (muscle isoform) deficiency is lethal in the mouse. Mol. Genet. Metab. 93, 314–322.

Keipert, S., Ost, M., Johann, K., Imber, F., Jastroch, M., van Schothorst, E.M., Keijer, J., Klaus, S., 2014. Skeletal muscle mitochondrial uncoupling drives endocrine cross-talk through the induction of FGF21 as a myokine. Am. J. Physiol. Endocrinol. Metab. 306, E469–E482.

Kharitonenkov, A., Shiyanova, T.L., Koester, A., Ford, A.M., Micanovic, R., Galbreath, E.J., Sandusky, G.E., Hammond, L.J., Moyers, J.S., Owens, R.A., et al., 2005. FGF-21 as a novel metabolic regulator. J. Clin. Invest. 115, 1627–1635.

Kim, K.H., Jeong, Y.T., Kim, S.H., Jung, H.S., Park, K.S., Lee, H.Y., Lee, M.S., 2013a. Metformin-induced inhibition of the mitochondrial respiratory chain increases FGF21 expression via ATF4 activation. Biochem. Biophys. Res. Commun. 440, 76–81.

Kim, K.H., Jeong, Y.T., Oh, H., Kim, S.H., Cho, J.M., Kim, Y.N., Kim, S.S., do, H, Kim, Hur, K.Y., Kim, H.K., et al., 2013b. Autophagy deficiency leads to protection from obesity and insulin resistance by inducing Fgf21 as a mitokine. Nat. Med. 19, 83–92.

Krauss, S., Zhang, C.Y., Lowell, B.B., 2005. The mitochondrial uncoupling-protein homologues. Nat. Rev. Mol. Cell Biol. 6, 248–261.

Lee, Y.H., Jung, Y.S., Choi, D., 2014. Recent advance in brown adipose physiology and its therapeutic potential. Exp. Mol. Med. 46, e78.

Lin, S.C., Li, P., 2004. CIDE-A, a novel link between brown adipose tissue and obesity. Trends Mol. Med. 10, 434–439.

Lo, S.C., Hannink, M., 2008. PGAM5 tethers a ternary complex containing Keap1 and Nrf2 to mitochondria. Exp. Cell Res. 314, 1789–1803.

Lu, W., Karuppagounder, S.S., Springer, D.A., Allen, M.D., Zheng, L., Chao, B., Zhang, Y., Dawson, V.L., Dawson, T.M., Lenardo, M., 2014. Genetic deficiency of the mitochondrial protein PGAM5 causes a Parkinson's-like movement disorder. Nat. Commun. 5, 4930.

Moriwaki, K., Farias Luz, N., Balaji, S., De Rosa, M.J., O'Donnell, C.L., Gough, P.J., Bertin, J., Welsh, R.M., Chan, F.K., 2016. The mitochondrial phosphatase PGAM5 is dispensable for necroptosis but promotes inflammasome activation in macrophages. J. Immunol. 196, 407–415.

Morrison, S.F., Madden, C.J., Tupone, D., 2014. Central neural regulation of brown adipose tissue thermogenesis and energy expenditure. Cell Metab. 19, 741–756.

Nishimura, T., Nakatake, Y., Konishi, M., Itoh, N., 2000. Identification of a novel FGF, FGF-21, preferentially expressed in the liver. Biochim. Biophys. Acta 1492, 203–206.

Owen, B.M., Mangelsdorf, D.J., Kliewer, S.A., 2015. Tissue-specific actions of the metabolic hormones FGF15/19 and FGF21. Trends Endocrinol. Metab. 26, 22–29.

Potthoff, M.J., Inagaki, T., Satapati, S., Ding, X., He, T., Goetz, R., Mohammadi, M., Finck, B.N., Mangelsdorf, D.J., Kliewer, S.A., et al., 2009. FGF21 induces PGC-1alpha and regulates carbohydrate and fatty acid metabolism during the adaptive starvation response. Proc. Natl. Acad. Sci. U. S. A. 106, 10853–10858.

Sekine, S., Kanamaru, Y., Koike, M., Nishihara, A., Okada, M., Kinoshita, H., Kamiyama, M., Maruyama, J., Uchiyama, Y., Ishihara, N., et al., 2012. Rhomboid protease PARL mediates the mitochondrial membrane potential loss-induced cleavage of PGAM5. J. Biol. Chem. 287, 34635–34645.

Sekine, Y., Zyryanova, A., Crespillo-Casado, A., Fischer, P.M., Harding, H.P., Ron, D., 2015. Stress responses. Mutations in a translation initiation factor identify the target of a memory-enhancing compound. Science 348, 1027–1030.

Sidrauski, C., Acosta-Alvear, D., Khoutorsky, A., Vedantham, P., Hearn, B.R., Li, H., Gamache, K., Gallagher, C.M., Ang, K.K., Wilson, C., et al., 2013. Pharmacological brake-release of mRNA translation enhances cognitive memory. eLife 2, e00498.

Takeda, K., Komuro, Y., Hayakawa, T., Oguchi, H., Ishida, Y., Murakami, S., Noguchi, T., Kinoshita, H., Sekine, Y., Iemura, S., et al., 2009. Mitochondrial phosphoglycerate mutase 5 uses alternate catalytic activity as a protein serine/threonine phosphatase to activate ASK1. Proc. Natl. Acad. Sci. U. S. A. 106, 12301–12305.

Tobiume, K., Matsuzawa, A., Takahashi, T., Nishitoh, H., Morita, K., Takeda, K., Minowa, O., Miyazono, K., Noda, T., Ichijo, H., 2001. ASK1 is required for sustained activations of JNK/p38 MAP kinases and apoptosis. EMBO Rep. 2, 222–228.

Townsend, K.L., Tseng, Y.H., 2014. Brown fat fuel utilization and thermogenesis. Trends Endocrinol. Metab. 25, 168–177.

Villarroya, F., Vidal-Puig, A., 2013. Beyond the sympathetic tone: the new brown fat activators. Cell Metab. 17, 638–643.

Wang, Z., Jiang, H., Chen, S., Du, F., Wang, X., 2012. The mitochondrial phosphatase PGAM5 functions at the convergence point of multiple necrotic death pathways. Cell 148, 228–243.

Westerberg, R., Mansson, J.E., Golozoubova, V., Shabalina, I.G., Backlund, E.C., Tvrdik, P., Retterstol, K., Capecchi, M.R., Jacobsson, A., 2006. ELOVL3 is an important component for early onset of lipid recruitment in brown adipose tissue. J. Biol. Chem. 281, 4958–4968.

Wikstrom, J.D., Mahdaviani, K., Liesa, M., Sereda, S.B., Si, Y., Las, G., Twig, G., Petrovic, N., Zingaretti, C., Graham, A., et al., 2014. Hormone-induced mitochondrial fission is utilized by brown adipocytes as an amplification pathway for energy expenditure. EMBO J. 33, 418–436.

Youle, R.J., Narendra, D.P., 2011. Mechanisms of mitophagy. Nat. Rev. Mol. Cell Biol. 12, 9–14.

Zhang, X., Yeung, D.C., Karpisek, M., Stejskal, D., Zhou, Z.G., Liu, F., Wong, R.L., Chow, W.S., Tso, A.W., Lam, K.S., et al., 2008. Serum FGF21 levels are increased in obesity and are independently associated with the metabolic syndrome in humans. Diabetes 57, 1246–1253.

Zhuang, M., Guan, S., Wang, H., Burlingame, A.L., Wells, J.A., 2013. Substrates of IAP ubiquitin ligases identified with a designed orthogonal E3 ligase, the NEDDylator. Mol. Cell 49, 273–282.